



Published by SET Publisher

Journal of Basic & Applied Sciences

ISSN (online): 1927-5129



Impact of Nano-FeS₂ Layer on the Stability Performance of CdS-Cu₂O PV Cells: A Study

Biswajit Ghosh*

The Neotia University, Kolkata, India

Article Info:

Keywords:

Nano structured FeS₂,
CdS-Cu₂O thin film PV Cell,
Stress stability performances.

Timeline:

Received: June 09, 2021

Accepted: July 06, 2021

Published: July 09, 2021

Citation: Ghosh B. Impact of Nano-FeS₂ Layer on the Stability Performance of CdS-Cu₂O PV Cells: A Study. J Basic Appl Sci 2021; 17: 64-70.

DOI: <https://doi.org/10.29169/1927-5129.2021.17.07>

Abstract:

The presence of nano-structured FeS₂ film at the junction of CdS-Cu₂O thin film PV cells demonstrated long term stability in its performances. The CdS layer was fabricated by vacuum evaporation technique and its top surface was converted to FeS₂ by dipping in hot FeCl₂ solution. The Cu₂O was deposited over it by plasma deposition process. A thin Ni-Au layer was deposited over the Cu₂O surface by an electroless deposition process to act as the top electrical contact. The cell properties and its stability were studied under external stresses including heat and light. The cells efficiency attained 2.35% at AM1 illumination. The fabricated cells were tested under thermal cycling and light soaking and their performances were compared with other cells like Si, CdTe and CIS. Results showed that the CdS-Cu₂O device with FeS₂ is more stable than the other cells. From these results it was concluded that the nano FeS₂ layer made perfect matching with n-CdS and p-Cu₂O due to its strong inversion and yields both bulk electrons and surface holes. Moreover, the hardness of the FeS₂ layer puts barriers that slow the inter-diffusion / migration of Cu ions into the bulk CdS thus preventing the formation of Cu-Cd killer centres.

*Corresponding Author
E-mail: bghosh3@gmail.com

© 2021 Biswajit Ghosh; Licensee SET Publisher.
This is an open access article licensed under the terms of the Creative Commons Attribution Non-Commercial License (<http://creativecommons.org/licenses/by-nc/3.0/>) which permits unrestricted, non-commercial use, distribution and reproduction in any medium, provided the work is properly cited.

1. INTRODUCTION

It was projected that by 2030 electricity from photovoltaic (PV) conversion will take a major share in the world electric power budget [1]. To achieve this goal, PV cells must be made up from earth-abundant, non-toxic, and air-stable materials. Today's PV market is mainly dominated by Si based PV cells; however, its energy payback period is comparatively higher than that of non-Si cells. Substantial efforts were made from 1955 in fabricating cheap non-Si based thin film PV cells for their successful commercial exploitation [2]. The thin films of chalcogenide compounds like CdS-Cu₂S were chosen as promising semiconducting materials in this venture due to their large natural abundance, low materials requirements and comparatively simple large scale fabrication process. The large scale fabrication process for this device was standardized and transferred to industry. However, after having more than 10% efficient cells, the structure was discarded due to their stability problems. Researchers reported that the major cause for degradation is due to transformation of the Cu₂S phase into a djurleite (Cu_{1.97}S) phase over time and the migration of Cu ions into the bulk of CdS leading to the formation of Cd-Cu carrier killer centres. Moreover, migration leads to the formation of shunt paths across the junction and the cell efficiencies is reduced by up to 60% [3]. To overcome this problem, Cu₂S in the CdS-Cu₂S structure was replaced by CdTe and CuInGaSe₂ and these cells appeared in the market. However, these cells still suffer from problems like long term stability and recyclability.

The djurleite phase may not be as detrimental to nano particle-based cells due to its high volume to surface energy [4]. Thus, particle-based PV cells may reduce the sensitivity to these effects by enabling rapid charge separation, but the nanoparticle morphology could also exacerbate phase instability according to reported research results [5]. Incorporation of additional earth-abundant hard cations with low diffusivity and solubility in other chalcogenides may be a possible solution to this. Incorporation of nano-structured iron pyrite (FeS₂) film into a CdS/Cu₂S junction is a possible solution to the stability of this structure. Although the conversion efficiency of FeS₂ based solar cells is less than 3%, the conductivity modulation properties in nano-structured FeS₂ [6] may be used in establishing the formation of a uniform p-n junction in the vicinity of CdS / FeS₂ / Cu₂S layers. This conductivity modulation may help the PV conversion activities across the CdS-Cu₂S junction.

In order to study the conductivity modulation properties of nano-structured FeS₂ films and its impact on PV conversion, a nano-structured FeS₂ layer was incorporated in the junction of CdS / Cu₂O films. The Cu₂O based PV device was fabricated using the structure of conducting glass / CdS / FeS₂ / Cu₂O / Ni-Au. The philosophy behind using the CdS / Cu₂O junction as chemical conversion of CdS surfaces into FeS₂ is comparatively easy than that of other processes and a thin layer of Cu₂O can be deposited over an FeS₂ layer either by physical or chemical deposition techniques.

Cuprous oxide (Cu₂O) is one of several candidate materials under consideration with the potential to reach 20% power conversion efficiency [7]. The material is p-type in nature and doping this material to make it n-type has proven to be challenging; thus, a common PV device architecture comprises a heterojunction structure with a partner from an earth abundant n-type material. Schottky barrier (SB) type Cu₂O based PV cells with efficiencies of 4.1% were fabricated by oxidizing Cu sheets at 110°C in air and thin film Cu₂O-ZnO based 1.3% PV cells were fabricated using an electrochemical deposition process [8, 9]. The open-circuit voltage (V_{OC}) of these devices is significantly below the theoretical limit of Cu₂O, due to a low built-in potential caused by non-ideal band alignment between the absorber and the window layer, and the generation of high recombination-current at the interface-traps [10].

FeS₂ is an earth abundant and inexpensive semiconducting material with low toxicity and it possesses a large density of surface states. The material was chosen as a possible candidate for solar energy conversion [11] owing to its suitable band gap (0.8–0.95 eV), high absorption coefficient (5-6 × 10⁵ cm⁻¹), and appropriate semiconducting properties [12]. Using this material, the best reported PV conversion efficiency remains below 3%. In this case, the researchers used single crystal pyrite in photo electrochemical (PEC) conversion systems [13]. The possible reason for low conversion was due to low V_{OC} (< 200 mV) and a low fill factor (FF) (< 0.5). The detailed studies reported that nano-structured and polycrystalline pyrite films are made of a degenerate p-type semiconductor [14] and showed no detectable photo-voltage. The possible reason for low V_{OC} is due to the surface Fermi level pinning in the middle of the bandgap induced due to enriched surface states [15]. The enriched surface states may originate from the loss

of sulphur ligands from the pyrite surfaces and have been recently re-examined by scanning tunnelling spectroscopy [16]. The Fermi level pinning possibly develops a sharp upward band bending induced by the surface states leading to the formation of a thin tunnelling region causing the low Voc [17].

Until today, no report is available on the use of surface inversion properties in perfect matching between the n and p semiconducting materials. In the present letter, a nano-structured FeS₂ layer was introduced in between the CdS and Cu₂O to study its impact on PV conversion as well its stability performance. This is the originality and novelty of this work.

In the present letter, a novel and new PV structure is reported where an Fe₂S layer was incorporated in between the n-CdS and p-Cu₂O layers and the PV properties were studied. The efficiency in these PV devices reached a level of 2.43%. The possible problems in achieving higher efficiencies are discussed.

2. EXPERIMENTAL TECHNIQUES

Thin films of CdS were deposited over commercially available ITO coated glass substrates by vacuum evaporation of electronic grade CdS powder from a tantalum effusion source. The ITO coated glass substrates were kept at 220°C during the deposition process. A ~1 µm thick CdS film was deposited on the ITO. The CdS coated substrates were then treated in hot FeCl₂ solution mixture containing 1.0 M of NH₄Cl, 0.07 M FeCl₂, and 0.24 M of N₂H₄, 2HCl. Before dipping in to the FeCl₂ solution, the CdS surface was etched for a minute in 5% HCl solution to activate the surface. The HCl activated surface was then dipped into the FeCl₂ solution at a temperature of 90°C and at a pH value of 6.5. The devices were dipped for a minute. The FeCl₂ treated surface was then dried and put it in oxygen plasma chamber for Cu₂O deposition.

The O₂ plasma was created by applying a DC electric potential across the three-ring type electrode system. The top and the bottom rings were connected to the negative terminal of the DC source, while the middle was connected to the positive terminal to confine the plasma in a cylindrical zone. Adjacent to the bottom electrode rings was a tantalum heating element to evaporate the metallic atoms and initiate their pass through the oxygen plasma zone. In the present case, pure Cu power or a Cu wire was used as the Cu source. The substrates were kept at close proximity to

the top electrode system. Initially the system was evacuated to 10⁻⁵ Torr, and then flashed with N₂ several times prior to the plasma generating system being energised. After the flashing operation, O₂ was introduced in to the chamber and the plasma system operated at a pressure of 10⁻¹-10⁻² Torr. A pink cylindrical plasma glow was observed surrounding the electrode zone. At stabilized plasma conditions, the tantalum heater source was energized and the Cu vapour was allowed to pass through the plasma zone. Under the influence of the DC potential, the Cu vapour gets ionized with the formation of Cu ions and in the presence of O₂ plasma, the Cu ions interacts with O₂ ions. Both the ions neutralized their charged state by depositing over the FeCl₂ treated CdS substrates. The deposited substrates were taken out and annealed at 210-220°C for 2-3 minutes to form the p-n junction device. Details of the fabrication process for Cu₂O films using plasma oxidation technique were reported in [18].

Electrical contact on the Cu₂O surface was fabricated using electroless deposition techniques involving Ni and Au, details of which are reported in reference [19]. To summarise, for the Ni electroless deposition process, the Cu₂O film was first treated with sensitizer solution, a mixture of SnCl₂ and HCl at room temperature. The sensitized surface was then treated in hot activator solution, a mixture of PdCl₂ and HCl, at 50°C. The composition of the electroless Ni bath was a mixture of NiSO₄, Na₂HPO₂, Na-Citrate and NH₄Cl. Deposition was conducted in pH 7-8 at 70-80°C for 3-4 minutes. After Ni deposition, Au was deposited over the Ni-surface. The electroless Au bath was a mixture of NaAuCl₄, Na₂SO₃, and Na₂B₄O₇. The deposition was carried out at 60-70°C at pH 8-9 for 2-3 minutes. The total thickness of the top contact was 30 nm. The photograph of CdS layer and the finished cell is presented in Figure 1 given below.

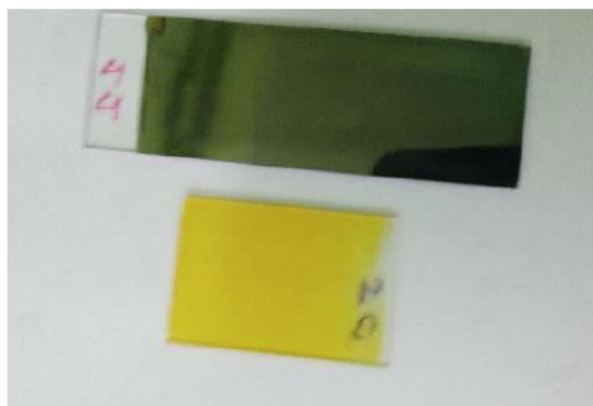


Figure 1: Photograph of CdS layer on ITO coated Glass (Bottom) and the total cell (Top).

Taking the ITO coating as the bottom contact and Au layer as the top contact, both dark and light characteristics of the device were recorded. For recording the light current-voltage (I-V) characteristics, the device was exposed to AM1 level of illumination from the bottom ITO side. The devices were then put under thermal stress cycling from -10°C to $+65^{\circ}\text{C}$ with a rate of 10°C per hour under continuous light exposure conditions at AM1 intensity.

The schematic diagram of each layer of the cell structure is presented in Figure 2a, and the photograph of test rig is also presented as Figure 2b, given below.

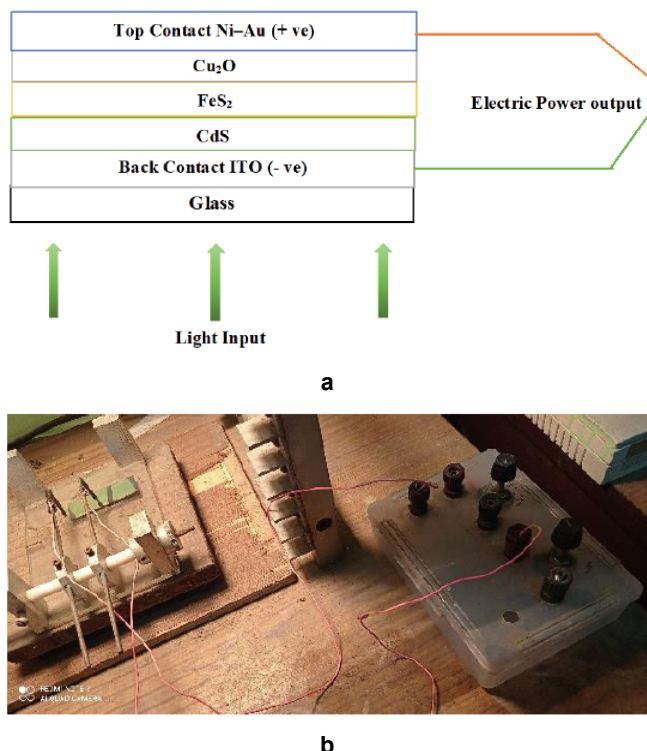


Figure 2: a. The schematic diagram of each layer of the cell structure. b. The test rig used to analyse the cell output.

3. RESULTS AND DISCUSSION

Both light and dark characteristics of the fabricated PV devices were recorded and are presented in Figure 3. From these characteristic curves, the figures of merit of the PV devices were extracted and showed a short circuit current density (J_{SC}) of 7.5 mA/cm^2 , an open circuit voltage (V_{OC}) of 0.575 V , and a fill factor (FF) / curve factor (CF) of 0.547 with the overall conversion efficiency (η) being 2.43% . Other extractable parameters are series resistance (R_{S}) of 18 Ohms , shunt resistance (R_{SH}) at 300 Ohm , diode factor (A) of the p-n junction device at dark condition of 2.4 and reverse saturation current (I_0) is of the order of 10^{-3} mA .

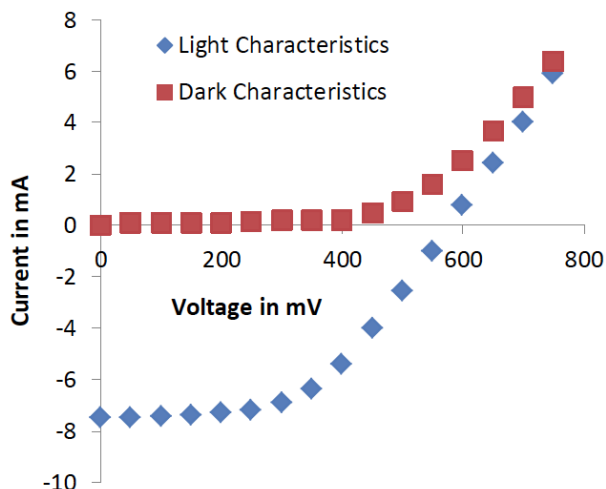


Figure 3: Dark and light I-V characteristic of CdS/FeS₂/Cu₂O cells.

The I-V characteristics were also recorded on applying light and thermal stress. The device without an FeS_2 layer with the structure of glass/ITO/CdS/ Cu_2O /Ni-Au was also fabricated without the step for conversion of CdS surface into an FeS_2 layer. Stability performances of both the cells were studied for six months by keeping them under ambient conditions. The results indicated that the cell without an FeS_2 layer degraded with time. The stability performances are presented in Figure 4. The normalized variation in figure of merits of the PV junction fabricated with materials like, Si, CdTe and CIS was estimated and is presented in Figures 3-6. The results indicate that under the influence of temperature stress in conjunction with light bias there were variations in PV conversion performance which returned back to its original figure after withdrawing the stresses. In addition, no hysteresis effect in the I-V characteristics was observed. The results were compared with the junction without the FeS_2 layer and also with multi-crystalline (mc) Si, CdS-CdTe and CdS-

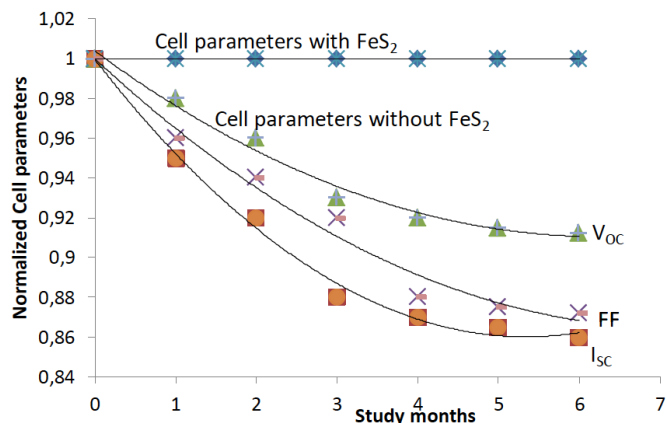


Figure 4: Stability performance of CdS/FeS₂/Cu₂O and CdS/Cu₂O PV cells with time.

CuInSe₂ (CIS) junctions to get an indication on the role of the FeS₂ layer in the junction during its operations under stressed and unstressed conditions.

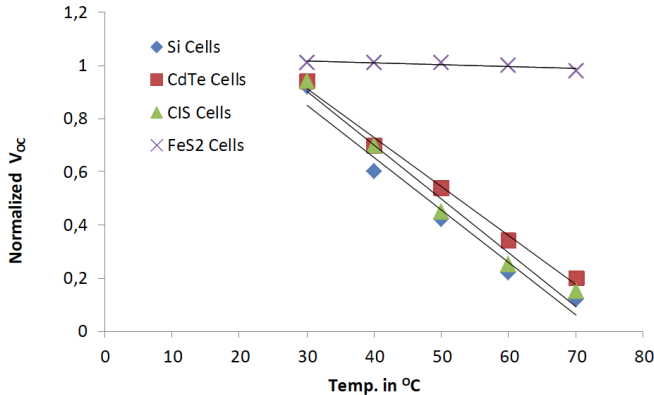


Figure 6: Variation of V_{OC} in various cells under temperature.

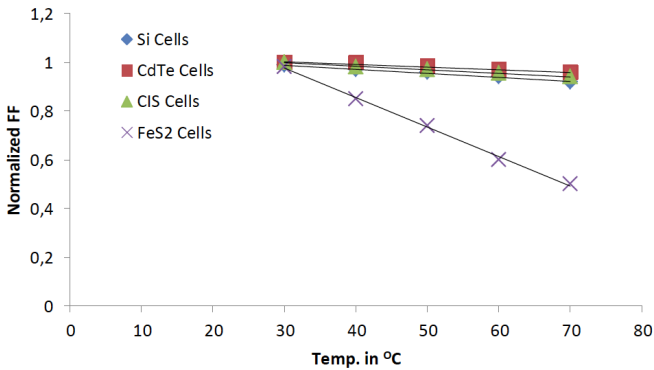


Figure 7: Variation of Fill Factor in various cells under temperature stress.

Researchers' report that FeS₂ based solar cells have efficiencies less than 2%. In the present case efficiency approached 2.5% due the photovoltaic activities occurring in the junction of the CdS/Fe₂S/Cu₂O layer where both the Fe₂S and Cu₂O layers have a role in photo conversion. In addition to photo conversion, it appears that the nano-structured FeS₂ layer has a prominent role in conductivity modulation which influences the matching of conductivities between the CdS-Cu₂O regions due to its surface inversion properties. The appropriate conductivity matching helps in forming an appropriate depletion across the junction boundaries that influences the carriers to migrate smoothly in the junction region. The R_s value of the fabricated device is quite high; this may be due to the surface properties of the Cu₂O layer. The values of the other parameters, like R_{sh}, J₀ and A, are in the appropriate range. The presence of the FeS₂ layer provides a barrier to the inter-diffusion / migration of Cd and Cu towards each other due to its hard nature. This inter-diffusion causes degradation and appears in

stressed CdS/Cu₂O junctions without this FeS₂ intermediate layer.

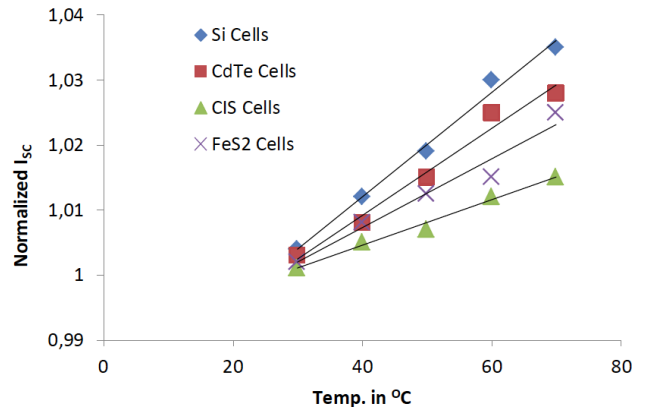


Figure 5: Variation of I_{SC} in various cells under temperature stress.

The normalized plot of the figures of merit of different PV cells presented in Figures 5-8 demonstrates the nature of FeS₂ in comparison to other materials. Figures 6 and 7 indicate some interesting information regarding the characteristics of the intermediated FeS₂ layer. In the variation of V_{OC} value with temperature, Figure 6 indicates that in case of FeS₂ cells there is little change in comparison to the other cells; however, the value of FF, as shown in Figure 7, changes drastically. The reason for stability of V_{OC} supports the stability of the FeS₂ layer which indicates no change in the R_{sh} value. In the case of FF, it appears that there is an increase in R_s value due to an increase in resistance of the FeS₂ layer with a rise in temperature. The total effect indicated that although there is a decrease in power out at elevated temperature, this tendency is lower than that experienced by the other cells, as shown in Figure 8.

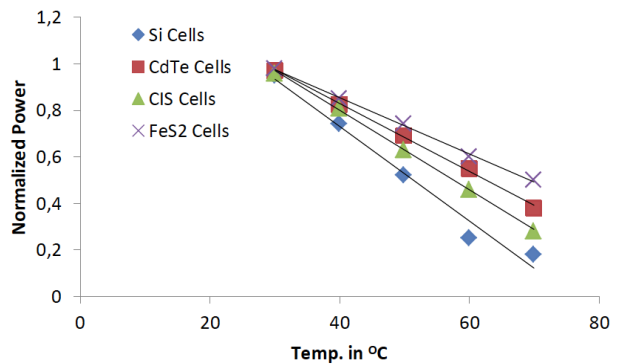


Figure 8: Variation of power output in various cells under temperature stress.

5. CONCLUSIONS

In conclusion, the improvement in stability of nano-structured CdS-Cu₂O PV devices due to the insertion

of a nano-structured FeS₂ layer at the CdS-Cu₂O junction has been demonstrated. From the experiments, it appears that photo generated carriers can flow smoothly from n - p region without major recombination due to the surface inversion properties of the intermediating FeS₂ layer. The FeS₂ layer also acts as the co-doping layer both at the n and p active interface which influences the donor ionization energies in the Cu₂O layer [20].

During light soaking and thermal cycling there is the possibility on the shrinkage in energy gaps of the semiconducting layers [21]. The thermal stress effect helps in the generation of additional carriers and at the same time this enhances their mobility due to thermal excitement.

Also observed was enhancement in the J_{SC} value. Due to the shrinkage in energy gap, the carriers required less energy to cross the built in potential. This has been reflected in the reduction in V_{OC} value. Shrinkage in the energy gap at the elevated temperature reduced the depletion layer width of the p-n junction and ultimately enhanced the shunt conductance created in reducing the V_{OC} value. Although at elevated temperature there was an increment in J_{SC}, this was not reflected in the R_S value, possibly due to reduction in conductance of the top metallic contact at the elevated temperature.

As the increment in J_{SC} was less than the decrement in V_{OC} value, a reduction in FF/CF was observed. In summary, the device efficiency η was reduced at the elevated temperature; however, the total performance reduction was less in comparison to other chalcogenide based thin film devices. On removal of stress, the device returned back in to its initial performance and no degradation in performance was observed as the FeS₂ layer is comparatively hard with the narrow energy gap behaving like a degenerate semiconductor.

The overall device efficiency remains low due to the large R_S value, this being attributed to the high bulk resistance of the active semiconductor. Further reduction in R_S value would be expected with appropriate doping. It is expected that the present experiments indicate a possible solution to addressing the degradation problem in chalcogenide based thin film PV cells. In conclusion, the present studies open up new avenues in studying stabilizing aspects in CdS based PV cells and informs on CdS-Cu₂S thin film structure design.

ACKNOWLEDGEMENTS

The author is grateful to the Council of Scientific and Industrial Research (CSIR), Govt. of India for providing funding support to work as the Emeritus Scientist at the School of Energy Studies, Jadavpur University.

REFERENCES

- [1] Devabhaktuni V, *et al.* Solar energy: Trends and enabling technologies. Renewable and Sustainable Energy Reviews 2013; 19: 555-564.
<https://doi.org/10.1016/j.rser.2012.11.024>
- [2] Chopra KL, *et al.* Thin Film Solar Cells. Plenum Press 1983.
<https://doi.org/10.1007/978-1-4899-0418-8>
- [3] Al-Dhafiri AM, *et al.* Degradation in CdS-Cu₂S photovoltaic cells. Semicond Sci Technol 1992; 7: 1052-1057.
<https://doi.org/10.1088/0268-1242/7/8/005>
- [4] Wu Y, *et al.* Synthesis and Photovoltaic Applications of Copper (I) Sulfide Nano crystals. Nano Lett 2008; 8: 2551-2555.
<https://doi.org/10.1021/nl801817d>
- [5] Lotfipour M, *et al.* α -Chalcocite Nanoparticle Synthesis and Stability. Chem Mater 2011; 23: 3032-3038.
<https://doi.org/10.1021/cm1031656>
- [6] Liang D, *et al.* Gated Hall Effect of Nanoplate Device Reveals Surface-State-Induced Surface Inversion in Iron Pyrite Semiconductor. Nano Lett 2014; 14: 6754-6760.
<https://doi.org/10.1021/nl501942w>
- [7] Nishi Y, *et al.* Effect of inserting a thin buffer layer on the efficiency in n-ZnO / p-Cu₂O heterojunction solar cells. J Vac Sci Technol A 2012; 30(4): 04D103 (1-6).
<https://doi.org/10.1116/1.3698596>
- [8] Karapety A, *et al.* Cuprous oxide thin films prepared by thermal oxidation of copper layer. Morphological and optical properties. J Luminescence 2015; 159: 325-332.
<https://doi.org/10.1016/j.jlumin.2014.10.058>
- [9] Nishi Y, *et al.* The impact of heterojunction formation temperature on obtainable conversion efficiency in n-ZnO-Cu₂O solar cells. Thin Solid Films 2013; 528: 72-76.
<https://doi.org/10.1016/j.tsf.2012.09.090>
- [10] Jeong S, *et al.* An analysis of temperature dependent current-voltage characteristics Cu₂O-ZnO heterojunction solar cells. Thin Solid Films 2011; 519: 6613-6619.
<https://doi.org/10.1016/j.tsf.2011.04.241>
- [11] Ennaoui A, *et al.* Iron disulphide for solar energy conversion. Sol Energy Mater Sol Cells 1993; 29: 289-270.
[https://doi.org/10.1016/0927-0248\(93\)90095-K](https://doi.org/10.1016/0927-0248(93)90095-K)
- [12] Ennaoui A, *et al.* Photoactive Synthetic Polycrystalline Pyrite (FeS₂). J Electrochem Soc 1985; 132(7): 1579-1582.
<https://doi.org/10.1149/1.2114168>
- [13] Lin YY, *et al.* Extended red light harvesting in a poly(3-hexylthiophene) / iron disulide nanocrystal hybrid solar cell. Nanotechnology 2009; 20.
<https://doi.org/10.1088/0957-4484/20/40/405207>
- [14] Berry N, *et al.* Atmospheric-Pressure Chemical Vapor Deposition of Iron Pyrite Thin Films. Adv Energy Mater 2012; 2: 1124-1135.
<https://doi.org/10.1002/aenm.201200043>
- [15] Ennaoui A, *et al.* In World Renewable Energy Congress. Energy and the Environment; A. A. M Sayigh, Ed.; Pergamon Press: Oxford 1990.
- [16] Herbert FW, *et al.* Quantification of electronic band gap and surface states on FeS₂ (100). Surf Sci 2013; 618: 53-61.
<https://doi.org/10.1016/j.susc.2013.08.014>

- [17] Bronold M, *et al.* Surface photovoltage measurement on pyrite (100) cleavage planes: Evidence for electronic bulk defects. *J Appl Phys* 1994; 76: 5800-5808.
<https://doi.org/10.1063/1.358393>
- [18] Santra K, *et al.* Copper Oxide thin films grown by plasma evaporation method. *Thin Solid Films* 1992; 213: 226.
[https://doi.org/10.1016/0040-6090\(92\)90286-K](https://doi.org/10.1016/0040-6090(92)90286-K)
- [19] Ghosh B. Electrical contacts for II-VI Semiconducting Devices. *Microelectronics Engineering* 2009; 86: 2187-2206.
<https://doi.org/10.1016/j.mee.2009.03.040>
- [20] Raebiger H, *et al.* Origins of the p-type nature and cation deficiency in Cu₂O and related materials. *Phys Rev* 2007; B76: 045209.
<https://doi.org/10.1103/PhysRevB.76.045209>
- [21] Olsen LC, *et al.* Explanation for low-efficiency Cu₂O Schottky-barrier solar cells. *Appl Phys Lett* 1979; 34: 47-49.
<https://doi.org/10.1063/1.90593>